

## On the mechanism of rapid metal exchange between thiolate-protected gold and gold/silver clusters: A time-resolved in situ XAFS study

Received 00th January 20xx,  
Accepted 00th January 20xx

DOI: 10.1039/x0xx00000x

www.rsc.org/

Bei Zhang,<sup>a\*</sup> Olga Safonova,<sup>b</sup> Stephan Pollitt,<sup>c</sup> Giovanni Salassa,<sup>a</sup> Annelies Sels,<sup>a</sup> Rania Kazan,<sup>a</sup> Yuming Wang,<sup>a</sup> Günther Rupprechter,<sup>c</sup> Noelia Barrabés,<sup>c\*</sup> Thomas Bürgi<sup>a</sup>

The fast metal exchange reaction between Au<sub>38</sub> and Ag<sub>x</sub>Au<sub>38-x</sub> nanoclusters in solution at -20°C has been studied by in situ X-ray absorption spectroscopy (time resolved quick EXAFS) in transmission mode. A cell was designed for this purpose consisting of a cooling system, remote injection and mixing devices. The capability of the set-up is demonstrated for second and minute time scale measurements of the metal exchange reaction upon mixing Au<sub>38</sub>/toluene and Ag<sub>x</sub>Au<sub>38-x</sub>/toluene solutions at both Ag K-edge and Au L<sub>3</sub>-edge. It has been proposed that the exchange of gold and silver atoms between the clusters occurs via the SR(-M-SR)<sub>n</sub> (n=1,2; M=Au, Ag) staple units in the surface of the reacting clusters during their collision. However, at no point during the reaction (before, during, after) evidence is found for cationic silver atoms within the staples. This means that either the exchange occurs directly between the cores of the involved clusters or the residence time of the silver atoms in the staples is very short in a mechanism involving the metal exchange within the staples.

### Introduction

Thiolate-protected gold and silver clusters are currently in the focus of scientific interest.<sup>1,2</sup> Their atomically precise structure makes them ideal model systems to study the evolution of structure as a function of cluster size, the properties of the gold (silver) thiolate interfaces<sup>3,4</sup> and the catalytic properties.<sup>5</sup> A rich variety of different cluster compositions has been reported in the last decade. The search for new cluster compounds mostly relies on x-ray crystallography,<sup>6</sup> mass spectrometry<sup>7,8</sup> and optical spectroscopy<sup>9</sup>. Some of the clusters are reported to be “extraordinary stable”, based on the observation that these compounds remain unchanged for days or weeks in solution, and even for much longer in the solid state. However, there is evidence that these clusters are rather dynamic molecular systems, where atoms can move between the sites but these transformations can be not evident as the average cluster structure often remains very similar or identical. It has for example been shown that thiolates in Au<sub>38</sub>(SR)<sub>24</sub> (SR: thiolate) clusters can move between

different symmetry distinct sites on the cluster surface.<sup>10</sup> Furthermore, the racemization of chiral Au<sub>38</sub>(SR)<sub>24</sub> evidences a drastic rearrangement of the SR-Au-SR-Au-SR (staple) units on the cluster surface, without any sign of decomposition of the cluster during this process.<sup>11</sup> The racemization of Au<sub>38</sub>(SR)<sub>24</sub> is observed at appreciable rate slightly above room temperature. It is influenced by Pd doping,<sup>12</sup> which reduces the racemization temperature. At the same time the incorporation of dithiolates within the ligand shell<sup>13</sup> leads to higher racemization temperatures. Gold – silver Au<sub>38-x</sub>Ag<sub>x</sub>(SR)<sub>24</sub> clusters also show highly dynamic behavior and , undergo racemization at room temperature.<sup>14</sup> Based on derived activation parameters it has been proposed that racemization could occur through consecutive reactions (S<sub>N</sub>2 type) between the staple units within the cluster, in which a sulfur atom within one staple attacks a gold atom in a neighboring staple.<sup>11</sup>

More recently it has been observed that metal atoms can exchange between thiolate-protected clusters at room temperature within minutes in solution. Using mass spectrometry Pradeep and coworkers reported the exchange of metal atoms and ligands between Au<sub>25</sub>(PET)<sub>18</sub> (PET: 2-phenylethylthiolate) and Ag<sub>44</sub>(FTP)<sub>30</sub> (FTP: 4-fluorothiophenol). In these experiments, Au<sub>25-x</sub>Ag<sub>x</sub>(PET)<sub>18-y</sub>(FTP)<sub>y</sub> were observed by mass spectrometry.<sup>15</sup> Similar processes were observed when mixing Au<sub>25</sub>(PET)<sub>18</sub> and Ag<sub>25</sub>(DMBT)<sub>18</sub> (DMBT: 2,4-dimethylbenzenethiolate).<sup>16</sup> Interestingly, the reaction between Au<sub>25</sub>(SR)<sub>18</sub> and Ag<sub>29</sub>(BDT)<sub>12</sub> (BDT: 1,3-benzenedithiolate) clusters resulted in metal exchange but not exchange of ligands, which was traced to the bidentate binding

<sup>a</sup> Department of Physical Chemistry, University of Geneva, 30 Quai Ernest-Ansermet, 1211 Geneva 4, Switzerland .

<sup>b</sup> Swiss Light Source, Paul Scherrer Institute, 5232 Villigen, Switzerland .

<sup>c</sup> Institut für Materialchemie, Technische Universität Wien, Getreidemarkt 9, 1060 Vienna, Austria

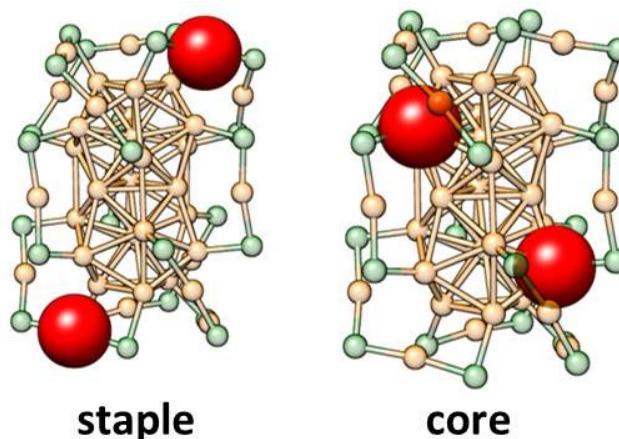
† Footnotes relating to the title and/or authors should appear here.

Electronic Supplementary Information (ESI) available: [details of any supplementary information available should be included here]. See DOI: 10.1039/x0xx00000x

mode of BDT.<sup>17</sup> Up to now the mechanism of this reaction remains unclear. Some of us have recently suggested that the metal exchange reaction between clusters takes place upon collisions rather than exchange of small species through solution, because separation of  $\text{Au}_{38}(\text{SR})_{24}$  and  $\text{Au}_{38-x}\text{Ag}_x(\text{SR})$  by a dialysis membrane completely prevented the reaction from occurring.<sup>18</sup> Based on mass spectrometry and theoretical calculations Pradeep and co-workers suggested the formation of a cluster dimer as an intermediate in the reaction.<sup>16</sup> In this structure a metal atom within a staple of one cluster is interacting with a sulphur atom within a staple of the other cluster and vice versa. This dimer intermediate is similar to the ones proposed to explain the racemization reaction mentioned above with the difference that in one case two staples located on different clusters react (metal exchange reaction), whereas in the other case staples on the same cluster are involved (racemization).<sup>11, 17</sup> During these reactions metal atoms and ligands can be exchanged between the staples.

The described highly dynamic nature of thiolate-protected clusters has of course important implications for any kind of application and it is therefore essential to better understand this reaction and its mechanism in more detail. The model described above implies that the exchange takes place via the staples however, up to now experimentally this issue remains open. Also, if the exchange takes place in the staples the metal atoms in the staples may further exchange with atoms within the cluster core. (See scheme 1 for staple and cluster core position of  $\text{Au}_{38}(\text{SR})_{24}$  cluster). Indeed, Pradeep and co-workers observed high numbers of metal atoms exchanged within one cluster, which implies that the exchange processes also involve the cluster core. If this indeed happens, i.e. if the metal atoms exchange between staples and then exchange within the core, what is the residence time of the atoms within the cluster staples? Addressing such questions requires special techniques. To shed some light on these questions, we have chosen the X-ray absorption spectroscopy (XAS). XAFS (X-ray absorption fine structure) spectroscopy is a powerful technique, which has been used to study the synthesis and catalytic properties of nanoparticles with high temporal resolution and site selectivity.<sup>19-23</sup> XAFS has been applied for understanding the local structure (coordination numbers and bond distances) of gold in pure and doped nanoclusters.<sup>20, 21</sup> These studies revealed the surface and core structure of gold nanoclusters,<sup>21</sup> its evolution during thermal treatments<sup>24</sup> and shed light on the position of heteroatom doped nanoclusters.<sup>25, 26</sup> XAFS measurements can be carried out either in transmission or fluorescence modes. Transmission mode is preferred over fluorescence due to shorter exposure time of nanoclusters to intense X-ray beams<sup>27, 28</sup> and higher signal-to-noise ratio allowing for better time resolution to probe their reactivity. Liquid phase XAFS measurements, however, have limits related to low sample concentration and absorption by the solvent. XAFS measurements in solution revealed the unique structure and bonding properties of metal nanoclusters,<sup>29</sup> which makes this technique promising for various operando studies including homogenous catalytic reactions.<sup>30</sup> The short staples are arranged along the equator

of the prolate core and the long staples form two triblade fans



at its ends. The dopant locations are in the staple and in the core of the nanocluster, red: dopant atom; yellow: Au; green: S. The organic part (R) is omitted for clarity.

Scheme 1. Structure of doped  $\text{Au}_{38}$  nanocluster. The cluster consists of a face-fused bi-icosahedral  $\text{Au}_{23}$  core which is protected by six dimeric (SR-Au-SR-Au-SR) and three monomeric (SR-Au-SR) staples. Stopped-flow and freeze quenching was used to study fast reactions in solution. To the best of our knowledge, no *in situ* time-resolved XAFS studies have been reported on the metal exchange between small nanoparticles in solution.

A key aspect of the presented *in situ* XAFS study on the silver migration mechanism concerns the cell design. *In situ* and *ex situ* cells/reactors have also been designed for liquid phase measurements, including windowless measurement reactor,<sup>33-35</sup> modified autoclaves,<sup>35</sup> microfluidic reactors,<sup>36</sup> or multidispenser-reactors<sup>31</sup>. In addition, stopped-flow and freeze quenching.

In addition, stopped-flow and freeze quenching were used to study fast reactions in solution.<sup>32</sup> When using the liquid cells for XAS in transmission mode, X-rays are transmitted through the liquid which is confined by two ultrathin windows. To the best of our knowledge, no *in situ* XAS studies have been reported on the reaction between two ultra-small nanoparticles in solution.

## Experimental

### Experimental Set-up

To study the fast metal exchange between thiolate-protected clusters in solution the liquid cell should meet the following specific requirements: (1) fast mixing of reactant solutions; (2) fast XAFS acquisition (3) adjustable cell length allowing to work in optimal conditions at different X-ray absorption edges and with different concentrations of solutions; (3) minimal sample exposure preventing X-ray beam damage; (4) possibility to cool the reaction solutions to slow down fast reactions.

The *in situ* system designed in this work comprises a syringe pump, a T mixer, a cooling gun and a liquid cell. Polytetrafluoroethylene (PTFE) tubing is used for the pump, T mixer as well as for connecting T mixer and liquid cell (Fig.1)

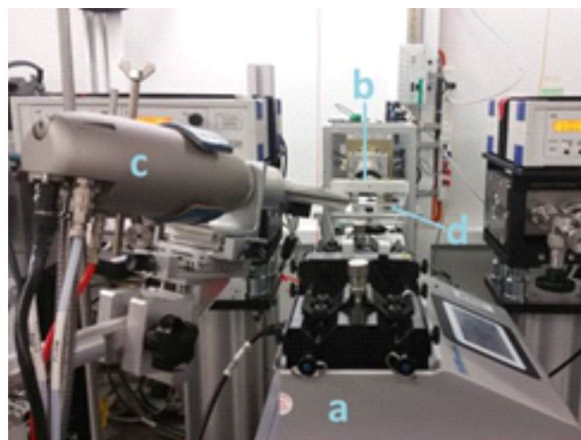
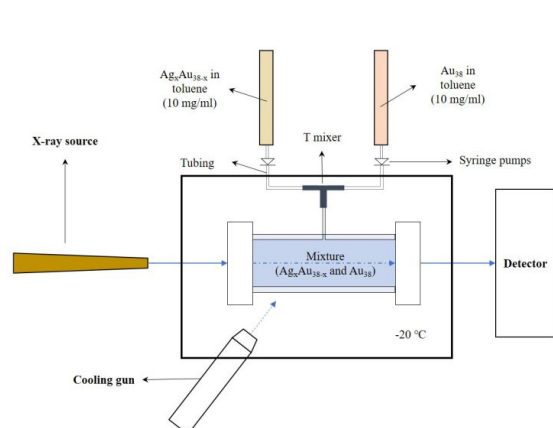


Figure 1. Schematic illustration and photo of the experimental set-up for the mechanism study of Ag migration between  $\text{Ag}_x\text{Au}_{38-x}$  and  $\text{Au}_{38}$  nanoclusters in solution: a. syringe pump; b. T mixer; c. cooling gun; d. liquid cell

To follow the reaction immediately after the mixing the two starting solutions containing two types of clusters, a remote-controlled syringe pump is employed.

Thin PTFE tubing (1/16" OD) is used to minimize the dead volume and to facilitate the solution mixing. The length of PTFE tubing between the T mixer and the cell is minimized at 7 cm. To slow down the silver migration reaction, the measurement cell was cooled down to  $-20\text{ }^\circ\text{C}$  using a cooling gun. In addition, after the fast mixing in the T mixer and filling of the cell, the reaction mixture was not stirred. To fill the cell a flow rate of 3 mL/min was used for both syringes.

The liquid cell design is schematically illustrated in Figure S1. The cell comprises a glass tube (OD 12 mm, ID 5 mm), which is sandwiched by two sets of a Teflon O ring (OD 12 mm, ID 7 mm), a Kapton window (thickness 0.76 mm, diameter 12 mm), a rubber O ring (OD 12 mm, ID 7 mm) and a metallic holder. A hole (diameter 3 mm) is made in the middle of the glass tube to fix the tubing and prevent overpressure upon liquid filling. All the units are fixed together by three screws that connect the metallic part on both ends. The thickness of the Kapton window takes into account the robustness of the material in the reactor and its absorption of X-rays. Transparent glass material is chosen for the cell to follow the reaction solution filling and the liquid level in the cell. The diameter and length of the glass tube were optimized based on calculations taking in account the theoretical absorption of each element along the beam path, such as the Kapton windows and the solvents that can have an effect on the cluster signal. The theoretical transmission with the optimal amount of nanoclusters, in the case of the two metals, was calculated from XAFSmass program<sup>37</sup>. Toluene is used as solvent for the measurement in order to obtain high cluster

concentration and low beam absorption. The length of the cell is adjusted for different measurements at Au L<sub>3</sub>-edge (10 mm) and Ag K-edge (30 mm). An advantage of this cell for studying the solution phase reaction between ultra-small nanoparticles is the facile set up and easily adjustable cell parameters.

#### In situ QEXAFS measurements

In situ time resolved quick XANES measurements<sup>38</sup> at the Ag K-edge (25.51 keV) and Au L<sub>3</sub>-edge (11.92 keV) of the silver migration reaction between  $\text{Ag}_x\text{Au}_{38-x}$  and  $\text{Au}_{38}$  in toluene were carried out at the SuperXAS beamline at the Swiss Light Source (Villigen, Switzerland).<sup>39</sup>  $\text{Ag}_x\text{Au}_{38-x}$  and  $\text{Au}_{38}$  samples were dissolved in toluene at a concentration of 10 mg/mL and loaded in the syringe pump. Before mixing, the cell was cooled down to  $-20\text{ }^\circ\text{C}$  by the cooling gun. Toluene solutions of  $\text{Ag}_x\text{Au}_{38-x}$  and  $\text{Au}_{38}$  were mixed in the T mixer and filled in the cell. A total volume of 0.6 mL and 0.13 mL was set for the measurements in Ag K-edge and Au L<sub>3</sub>-edge respectively. Low solution volumes are crucial for the measurements as the purified samples are precious. The spectra were measured in transmission mode using ionization chambers as detectors. Channel cut Si(311) and Si(111) monochromators, were used to measure XAFS spectra at Ag K-edge and Au L<sub>3</sub>-edge, respectively. For Ag K-edge measurements we used Pt-coated mirrors at 2.5 mrad and for Pt L<sub>3</sub> edge we used Rh coated mirrors at 2.5 mrad. Quick XAFS (QXAFS) measurements were started before the mixed solution reached the cell and were continued for 30 min acquiring 1000 eV XAFS spectrum every 0.1 s for Ag K-edge and every 1s for Au L<sub>3</sub>-edge. After starting the pump injection, the two starting solutions are mixed at the M,L mixer and filled the cell within 3 s before the first stable spectrum was obtained. As references, the QXAFS spectra

of pure solutions of  $\text{Ag}_x\text{Au}_{38-x}$  and  $\text{Au}_{38}$  nanoclusters were recorded in the same cell and the same conditions. All XAFS spectra were background subtracted and normalized to the edge jump of 1 following standard procedures using Demeter software.<sup>40</sup>

### Sample Synthesis

All chemicals were used as received.  $\text{Au}_{38}(\text{SR})_{24}$  (-SR=PET, -SR is omitted below for simplicity) was synthesized by thermal etching of polydispersed  $\text{Au}_n(\text{SG})_m$  nanoclusters prepared from Brust method with phenylethanethiol.<sup>41</sup>  $\text{Ag}_x\text{Au}_{38-x}$  was obtained from metal exchange between  $\text{Au}_{38}$  and AgSR, according to a recent protocol.<sup>14</sup> The purity of  $\text{Au}_{38}$  and  $\text{Ag}_x\text{Au}_{38-x}$  ( $x$  refers to the Ag dopant number in  $\text{Ag}_x\text{Au}_{38-x}$  sample) was confirmed by MALDI-TOF mass spectrometry using a Bruker Autoflex mass spectrometer equipped with a nitrogen laser at near threshold laser fluence in positive linear mode. Trans-2-[3-(4-tert-Butylphenyl)-2-methyl-2-propenylidene] malononitrile was used as the matrix with a 1:1.000 analyte:matrix ratio. A volume of 2  $\mu\text{l}$  of the analyte/matrix mixture was applied to the target and air-dried.

### Results and Discussion

Figure 2 shows the MALDI mass spectra of the  $\text{Ag}_x\text{Au}_{38-x}$  and  $\text{Au}_{38}$  nanocluster samples used for the XAS measurements. Whereas the  $\text{Au}_{38}$  sample contains a single species the  $\text{Ag}_x\text{Au}_{38-x}$  sample is a mixture of several species differing in the number  $x$  of silver atoms replacing gold in the cluster. As can be seen from Figure 2  $x$  ranges from 1 to 10 with a maximum around 8. Note that Dass and coworkers were able to crystallize  $\text{Ag}_x\text{Au}_{38-x}$  clusters and they found that the silver atoms preferentially occupy nine positions within the 23 atom core of the cluster, namely the two vertex edges (three atoms on each edge) and the middle face-shared three-atom ring (see Scheme 1).<sup>42</sup> Our XAFS spectra of  $\text{Ag}_x\text{Au}_{38-x}$  (see below) also indicate core positions of the Ag atoms. Observe that the core atoms at the vertex edges bind to the sulfur atom of the dimeric SR-Au-SR-Au-SR staples.

Fig. 3 shows the Au  $L_3$ -edge XANES of the reaction mixture of  $\text{Ag}_x\text{Au}_{38-x}$  and  $\text{Au}_{38}$  nanoclusters. The spectra of  $\text{Ag}_x\text{Au}_{38-x}$  and  $\text{Au}_{38}$  references were averaged over 10 min. Good quality XANES spectra were achieved already for 1s acquisition time, revealing the power of the cell and experimental approach. Compared to metallic gold foil, the white line positions of  $\text{Au}_2\text{S}$ ,  $\text{AuCl}$  and  $\text{AuCl}_3$ , exhibit energy shift of 1 eV, -2 eV and -2.5 eV, respectively.<sup>43</sup> However, we observed no changes in the edge position. Also the white line intensity remained unchanged during the first 3s of reaction between  $\text{Ag}_x\text{Au}_{38-x}$  and  $\text{Au}_{38}$  nanoclusters and also after longer times. In comparison to the reference samples

( $\text{Au}_{38}$  and  $\text{Ag}_x\text{Au}_{38-x}$ ), the XANES spectra do not change much during reaction. This insensitivity can be related to the fact that XANES spectra represent an average of Au atoms in different oxidation states, related to core and staple positions (Scheme 1). During the Ag migration process, both metallic (core) and oxidized charged states (staple) of Au atoms exist in the reaction mixture. The ratio between metallic and oxidized states could vary during the reaction depending on the position of the Au atoms in the clusters (core vs. staple).

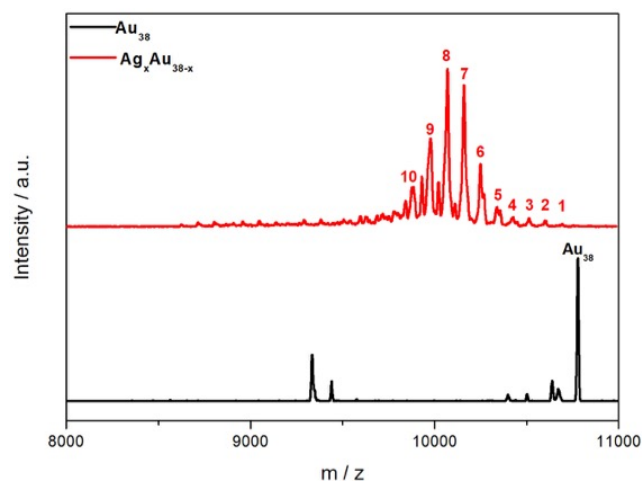
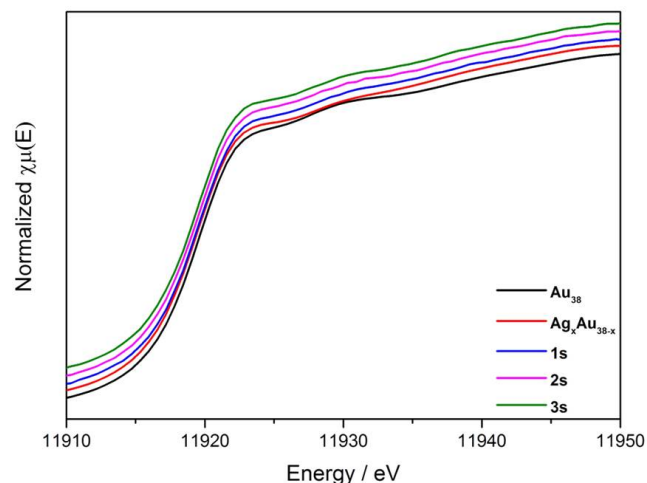


Figure 2. MALDI spectra of  $\text{Ag}_x\text{Au}_{38-x}$  and  $\text{Au}_{38}$  nanoclusters. The dopant numbers  $x$  in  $\text{Ag}_x\text{Au}_{38-x}$  sample are marked at the corresponding peak.



Some fragmentation peaks were also observed in both samples.

Figure 3. In situ XANES spectra at Au  $L_3$ -edge of the silver migration reaction. The spectra were stacked for clarity. Shown are the spectra of the initial  $\text{Ag}_x\text{Au}_{38-x}$  and  $\text{Au}_{38}$  samples as well as of the reaction mixture after 1 second, 2 seconds and 3 seconds of reaction. Note that time zero was set at the time where the first stable XAS spectrum was measured, i.e. when the liquid level in the cell covered the X-ray beam path.

Fig. 4 shows the XANES of the reaction mixture at Ag  $K$ -edge. The XANES of Ag foil, the starting  $\text{Ag}_x\text{Au}_{38-x}$  and the reaction mixture after 10 min are shown in Fig. 4a.

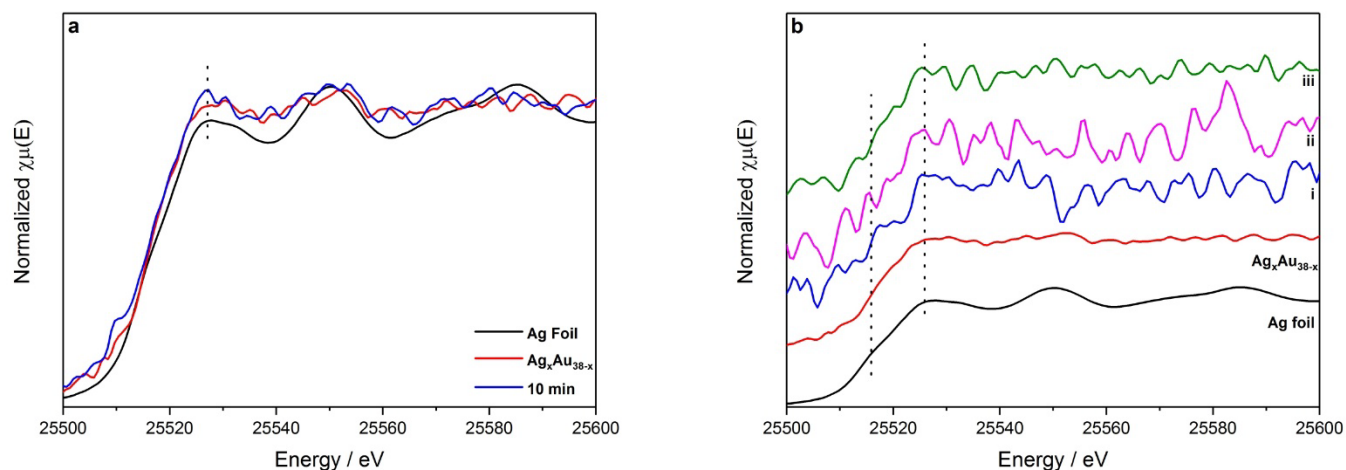


Figure 4. XANES spectra of the silver migration reaction at Ag K-edge: a. starting ( $\text{Ag}_x\text{Au}_{38-x}$  nanocluster before reaction) and final ( $t=10$  min) reaction solution. The spectrum at 10 min was obtained by averaging the recorded spectra over 45 s. b. in situ spectra at the beginning of the reaction. The recorded spectra were averaged every 15 s, the corresponding reaction time is shown on the right: i. 0-15s, ii. 15-30s, iii. 30-45s. Figure 4b is stacked for clarity.

The quality of the XANES spectra at the Ag K-edge is not as good as the one for the Au  $L_3$ -edge shown above. The main reason for this is the low silver concentration and absorption by the solvent. We therefore averaged over 45 seconds in order to obtain a XANES spectrum of reasonable quality for the reaction mixture 10 minutes after mixing. Note that Ag migration from  $\text{Ag}_x\text{Au}_{38-x}$  to  $\text{Au}_{38}$  under these conditions should occur within 10 min (or faster) according to our previous study.<sup>18</sup>

Compared to the Ag foil, the  $\text{Ag}_x\text{Au}_{38-x}$  sample shows slightly higher Ag K-edge white line intensity and broadening of the first peak above the edge, which is in agreement with the reported XANES of  $\text{Au}_{98}\text{Ag}_{46}$  nanocluster.<sup>44</sup> No representative energy edge shift was observed between the starting  $\text{Ag}_x\text{Au}_{38-x}$  sample and the sample after 10 min of the reaction, indicating similar Ag location and implying that the Ag remains in the core position in the nanocluster (Scheme 1), in agreement with X-ray crystallography.<sup>42</sup> In the compounds containing cationic silver, such as  $\text{Ag}_2\text{S}$ ,  $\text{AgCl}$ , Ag-thiol or Ag-glutathione, the Ag K-edge XANES spectra show obvious shifts in the positions and intensities of the white line and other peaks above the edge in comparison to Ag foil (Figure S3 and S4).<sup>45-49</sup> For Ag atoms forming covalent bond with S the white line systematically shifts to lower energies (Figure S4). The slight shift in the Ag K-edge XANES of the  $\text{Ag}_x\text{Au}_{38-x}$  sample before and after reaction is rather positive, which suggests Ag is not abundantly present in the staple positions (Figure S4). To track possible reaction intermediates, the Ag exchange reaction was also followed by the Ag K-edge XANES during the first 45 s (shown the Fig. 4b). The spectra were averaged over 15 s due to the low data quality. If Ag atoms temporarily migrate to the staples to form  $\text{S}-(\text{M}-\text{S})_n$  ( $n=1, 2$ ; M: Ag or Au) bonds, one should expect formation of cationic Ag and corresponding shift and intensity change of the Ag K-edge white line. However, no significant changes in the white line was observed after 15, 30 and 45 s of the reaction.

To summarize, the XAS spectra presented above reveal that (i) the silver atoms are located in the core of the  $\text{Ag}_x\text{Au}_{38-x}$  starting cluster and (ii) at no point during the reaction (within experimental time resolution) an indication of silver atoms within the staples can be found. In the context of previous findings, namely that the metal exchange is taking place during collisions between clusters rather than exchange of small species through solution<sup>15</sup> the current results are consistent with two scenarios: (1) Ag migrates directly from the core  $\text{Ag}_x\text{Au}_{38-x}$  to the core of  $\text{Au}_{38}$  (and Au concomitantly in the opposite direction) without passing through the nanocluster staple. (2) The lifetime of possible staple Ag intermediates are too short and therefore their concentration too low to be detected. Note that in a consecutive reaction ( $\text{A} \rightarrow \text{B} \rightarrow \text{C}$ ) the concentration of the intermediate species (B) depends on the relative rate constants for the two reactions ( $\text{A} \rightarrow \text{B}$  and  $\text{B} \rightarrow \text{C}$ ). The concentration of the intermediate will be very low if the second reaction is much faster than the first one. Translated to scenario (2) this means the following: Formation of Ag in staple positions (intermediate) through a collision between clusters is slow compared to the migration of Ag from staple to core position within a cluster. Considering that the metal exchange reaction is fast, as confirmed by several studies, the migration of silver atoms from staple to core positions is even faster.

Up to now there is no direct information available, which would allow one to discriminate between the two scenarios mentioned above. However, direct exchange of core atoms during collision (scenario (1)) seems unlikely in view of the steric requirements imposed by the ligand shell. Exchange of metal atoms between staples seems more likely. The current measurements therefore indicate that the residence time of the Ag atoms in the staples is very short, meaning that exchange within the cluster, between staple and core sites, is fast.

In order to verify that the silver migration reaction occurred under the QXAFS measurement conditions, the reaction mixture was collected after in situ measurements

from both Au L<sub>3</sub>-edge and Ag K-edge experiments. The highly doped Ag<sub>x</sub>Au<sub>38-x</sub> species (x=9, 10) in the starting sample disappeared. Instead, the reacted mixture showed new Ag<sub>x</sub>Au<sub>38-x</sub> species with Ag dopant number from 0 to 8. Redistribution of the silver atoms is therefore confirmed and most obvious by comparing MALDI spectra of the samples after reaction (Figure 5) with the one of the initial Ag<sub>x</sub>Au<sub>38-x</sub> sample (Figure 2).

The average number of silver atoms in Ag<sub>x</sub>Au<sub>38-x</sub> clusters before the Ag migration reaction was 7.5. During the Ag migration experiment the Ag<sub>x</sub>Au<sub>38-x</sub> cluster was mixed with Au<sub>38</sub> in the 1:1 ratio and therefore, the average x after the reaction should be a half of the value for the initial Ag<sub>x</sub>Au<sub>38-x</sub> sample. Nevertheless, after *in situ* XAS measurements at Ag K- and Au L<sub>3</sub>-edges MALDI indicated the average number of silver atoms of 2.8 and 2.5, respectively. The discrepancy between the experimental and theoretical values may be due to the several reasons including small errors in weighting and addition of volumes to the cell. We believe the main reason however, is related to the laser intensity in the MALDI process causing more pronounced fragmentation of highly doped Au<sub>38</sub> nanoclusters in comparison to the lower doped ones.

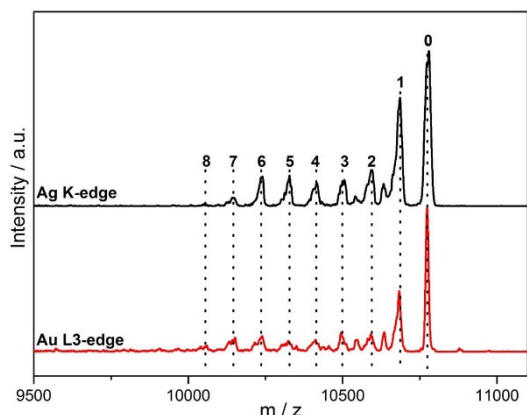


Figure 5. MALDI spectra of the reaction solution after *in situ* measurement at Au L<sub>3</sub>-edge and Ag K-edge. Ag dopant number is marked for each species.

## Conclusions

We report a novel *in situ* set-up for time-resolved transmission QXAFS studies of chemical reactions in solution on second and minute time scales. The simple and adjustable components of the set-up make it suitable for mechanistic studies of different reactions in solution. It is particularly suited for fast reactions due to the low dead time of solution mixing and filling the cell in only 3s. Using this setup we studied the mechanism of silver migration in thiolate protected gold clusters. Good data quality has been obtained in Au L<sub>3</sub>-edge XANES with a time resolution of 1s, whereas the XANES spectra recorded at Ag K-edge had lower quality and at least 45 s required for reliable chemical speciation.

The experiments show that at no time (before and during the reaction between Ag<sub>x</sub>Au<sub>38-x</sub> and Au<sub>38</sub> clusters in solution) silver atoms are found in significant amounts within the staples. This means that either the metal

exchange occurs directly between core sites or, if the exchange happens between metal atoms within the staple, that the residence time of the silver in the staples is very short and therefore its concentration low. Further experiments are needed to discriminate between these two scenarios.

## Acknowledgements

Generous support by the University of Geneva and the Swiss National Science Foundation (Grant number 200020\_152596) is acknowledged. We thank Patrick Barman for help in building the cell. We thank the Paul Scherrer Institute for providing beam time at SuperXAS beamline of the Swiss Light Source (SLS20161450). SP and GR acknowledge the Austrian Science Fund (FWF, project I1041-N28 COMCAT) We also acknowledge the contributions of the Sciences Mass Spectrometry (SMS) platform at the Faculty of Sciences, University of Geneva.

## Notes and references

1. R. C. Jin, C. J. Zeng, M. Zhou and Y. X. Chen, *Chem Rev*, 2016, **116**, 10346-10413.
2. I. Chakraborty and T. Pradeep, *Chem. Rev.*, 2017, **117**, 8208-8271.
3. H. Hakkinen, *Nat. Chem.*, 2012, **4**.
4. T. Burgi, *Nanoscale*, 2015, **7**, 15553-15567.
5. G. Li and R. C. Jin, *Accounts Chem. Res.*, 2013, **46**, 1749-1758.
6. P. D. Jadzinsky, G. Calero, C. J. Ackerson, D. A. Bushnell and R. D. Kornberg, *Science*, 2007, **318**, 430-433.
7. T. G. Schaaff, M. N. Shafiqullin, J. T. Khoury, I. Vezmar, R. L. Whetten, W. G. Cullen, P. N. First, C. GutierrezWing, J. Ascensio and M. J. JoseYacaman, *J. Phys. Chem. B*, 1997, **101**, 7885-7891.
8. A. Dass, A. Stevenson, G. R. Dubay, J. B. Tracy and R. W. Murray, *J. Am. Chem. Soc.*, 2008, **130**, 5940-5946.
9. T. G. Schaaff and R. L. Whetten, *J. Phys. Chem. B*, 2000, **104**, 2630-2641.
10. L. Beqa, D. Deschamps, S. Perrio, A. C. Gaumont, S. Knoppe and T. Burgi, *J Phys Chem C*, 2013, **117**, 21619-21625.
11. S. Knoppe, I. Dolamic and T. Burgi, *J. Am. Chem. Soc.*, 2012, **134**, 13114-13120.
12. N. Barrabes, B. Zhang and T. Burgi, *Journal of the American Chemical Society*, 2014, **136**, 14361-14364.
13. S. Knoppe, S. Michalet and T. Burgi, *J. Phys. Chem. C*, 2013, **117**, 15354-15361.
14. B. Zhang and T. Burgi, *J Phys Chem C*, 2016, **120**, 4660-4666.

15. K. R. Krishnadas, A. Ghosh, A. Baksi, I. Chakraborty, G. Natarajan and T. Pradeep, *J. Am. Chem. Soc.*, 2016, **138**, 140-148.
16. K. R. Krishnadas, A. Baksi, A. Ghosh, G. Natarajan and T. Pradeep, *Nat. Commun.*, 2016, **7**, 9.
17. K. R. Krishnadas, A. Baksi, A. Ghosh, G. Natarajan, A. Som and T. Pradeep, *Accounts Chem. Res.*, 2017, **50**, 1988-1996.
18. B. Zhang, G. Salassa and T. Burgi, *ChemComm*, 2016, **52**, 9205-9207.
19. D. Koziej, *Chem Mater*, 2016, **28**, 2478-2490.
20. D. M. Chevrier, R. Yang, A. Chatt and P. Zhang, *Nanotechnol Rev*, 2015, **4**, 193-206.
21. P. Zhang, *J Phys Chem C*, 2014, **118**, 25291-25299.
22. R. Ishida, S. Hayashi, S. Yamazoe, K. Kato and T. Tsukuda, *J. Phys. Chem. Lett.*, 2017, **8**, 2368-2372.
23. S. Yamazoe, S. Takano, W. Kurashige, T. Yokoyama, K. Nitta, Y. Negishi and T. Tsukuda, *Nat. Comm.*, 2016, **7**, 10414.
24. B. Zhang, S. Kaziz, H. Li, M. G. Hevia, D. Wodka, C. Mazet, T. Burgi and N. Barrabes, *J Phys Chem C*, 2015, **119**, 11193-11199.
25. S. Sharma, S. Yamazoe, T. Ono, W. Kurashige, Y. Niihori, K. Nobusada, T. Tsukuda and Y. Negishi, *Dalton T*, 2016, **45**, 18064-18068.
26. B. Zhang, S. Kaziz, H. H. Li, D. Wodka, S. Malola, O. Safonova, M. Nachtegaal, C. Mazet, I. Dolamic, J. Llorca, E. Kalenius, L. M. L. Daku, H. Hakkinen, T. Burgi and N. Barrabes, *Nanoscale*, 2015, **7**, 17012-17019.
27. M. Nagasaka, H. Yuzawa, T. Horigome and N. Kosugi, *Rev Sci Instrum*, 2014, **85**.
28. C. Schwanke, L. F. Xi and K. M. Lange, *J Synchrotron Radiat*, 2016, **23**, 1390-1394.
29. M. A. MacDonald, P. Zhang, N. Chen, H. F. Qian and R. C. Jin, *J Phys Chem C*, 2011, **115**, 65-69.
30. G. J. Sherborne and B. N. Nguyen, *Chem. Cent. J.*, 2015, **9**.
31. J. Boita, M. V. Castegnaro, M. D. M. Alves and J. Morais, *J Synchrotron Radiat*, 2015, **22**, 736-744.
32. S. A. Bartlett, J. Moulin, M. Tromp, G. Reid, A. J. Dent, G. Cibin, D. S. McGuinness and J. Evans, *ACS Catal.*, 2014, **4**, 4201-4204.
33. S. G. Booth, A. Uehara, S. Y. Chang, J. F. W. Mosselmans, S. L. M. Schroeder and R. A. W. Dryfe, *J Phys Chem C*, 2015, **119**, 16785-16792.
34. J. D. Cafun, K. O. Kvashnina, E. Casals, V. F. Puentes and P. Glatzel, *Acs Nano*, 2013, **7**, 10726-10732.
35. J. D. Grunwaldt, M. Ramin, M. Rohr, A. Michailovski, G. R. Patzke and A. Baiker, *Rev Sci Instrum*, 2005, **76**.
36. A. M. Karim, N. Al Hasan, S. Ivanov, S. Siefert, R. T. Kelly, N. G. Hallfors, A. Benavidez, L. Kovarik, A. Jenkins, R. E. Winans and A. K. Datye, *J Phys Chem C*, 2015, **119**, 13257-13267.
37. K. Klementiev and R. Chernikov, *J. Phys. Conf. Ser.*, 2016, **712**, 012008.
38. O. Muller, M. Nachtegaal, J. Just, D. Lutzenkirchen-Hecht and R. Frahm, *J. Synchrot. Radiat.*, 2016, **23**, 260-266.
39. P. M. Abdala, O. V. Safonova, G. Wiker, W. van Beek, H. Emerich, J. A. van Bokhoven, J. Sa, J. Szlachetko and M. Nachtegaal, *Chimia*, 2012, **66**, 699-705.
40. B. Ravel and M. Newville, *J Synchrotron Radiat*, 2005, **12**, 537-541.
41. H. F. Qian, Y. Zhu and R. C. Jin, *Acs Nano*, 2009, **3**, 3795-3803.
42. C. Kumara, K. J. Gagnon and A. Dass, *J Phys Chem Lett*, 2015, **6**, 1223-1228.
43. A. Demortiere, R. D. Schaller, T. Li, S. Chattopadhyay, G. Krylova, T. Shibata, P. C. D. Claro, C. E. Rowland, J. T. Miller, R. Cook, B. Lee and E. V. Shevchenko, *J. Am. Chem. Soc.*, 2014, **136**, 2342-2350.
44. J. Liu, K. S. Krishna, C. Kumara, S. Chattopadhyay, T. Shibata, A. Dass and C. S. S. R. Kumar, *RSC Adv.*, 2016, **6**, 25368-25374.
45. N. V. Hudson-Smith, P. L. Clement, R. P. Brown, M. O. P. Krause, J. A. Pedersen and C. L. Haynes, *Environ Sci-Nano*, 2016, **3**, 1236-1240.
46. G. Veronesi, A. Deniaud, T. Gallon, P. H. Jouneau, J. Villanova, P. Delangle, M. Carriere, I. Kieffer, P. Charbonnier, E. Mintz and I. Michaud-Soret, *Nanoscale*, 2016, **8**, 17012-17021.
47. G. Veronesi, C. Aude-Garcia, I. Kieffer, T. Gallon, P. Delangle, N. Herlin-Boime, T. Rabilloud and M. Carriere, *Nanoscale*, 2015, **7**, 7323-7330.
48. R. Kaegi, A. Voegelin, B. Sinnet, S. Zuleeg, H. Hagendorfer, M. Burkhardt and H. Siegrist, *Environ. Sci. Technol.*, 2011, **45**, 3902-3908.
49. C. L. Doolette, M. J. McLaughlin, J. K. Kirby, D. J. Batstone, H. H. Harris, H. Ge and G. Cornelis, *Chem. Cent. J.*, 2013, **7**, 46-46.

## Supporting Information

### On the mechanism of rapid metal exchange between thiolate-protected gold and gold/silver clusters: A time-resolved *in situ* XAFS study

Bei Zhang,<sup>a\*</sup> Olga Safonova,<sup>b</sup> Stephan Pollitt,<sup>c</sup> Giovanni Salassa,<sup>a</sup> Annelies Sels,<sup>a</sup> Rania Kazan,<sup>a</sup> Yuming Wang,<sup>a</sup> Günther Rupprechter,<sup>c</sup> Noelia Barrabés,<sup>c\*</sup> Thomas Bürgi<sup>a</sup>

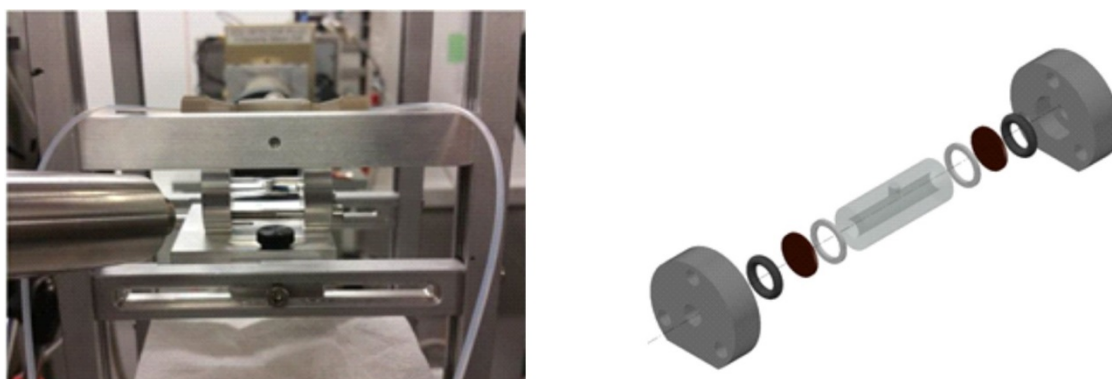


**Figure S1.** Photos and schematic illustration of the cell for the *in situ* studies.

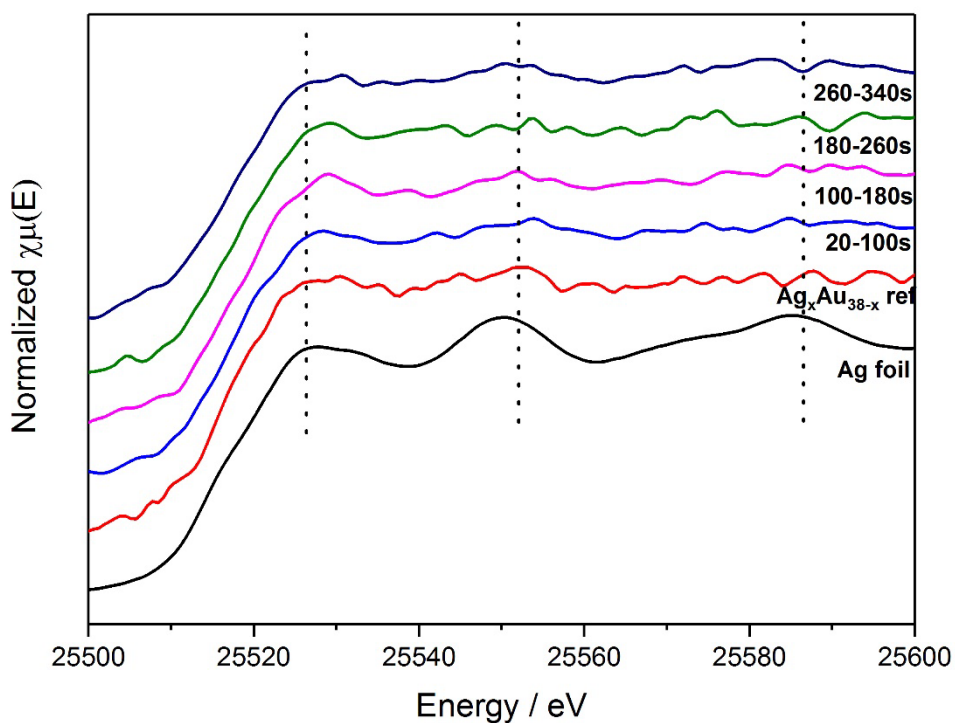


**Figure S2.** XANES spectra of the silver migration reaction at Ag K-edge at longer reaction times

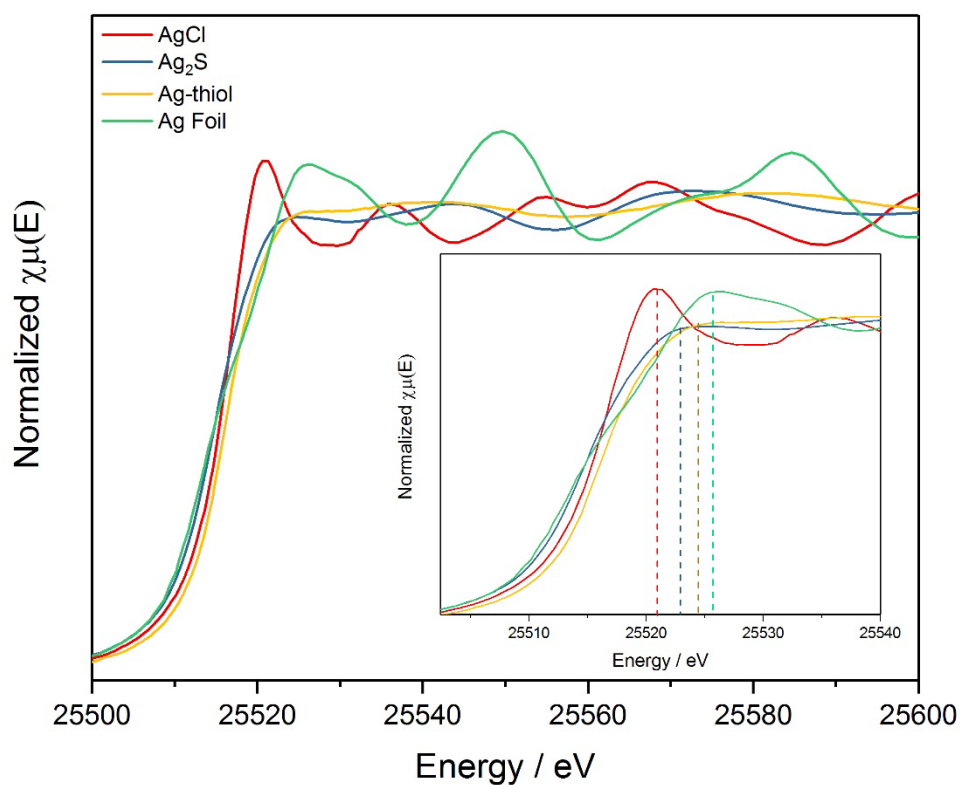


**Figure S3.** XANES spectra of silver references at Ag K-edge from ref <sup>1</sup>

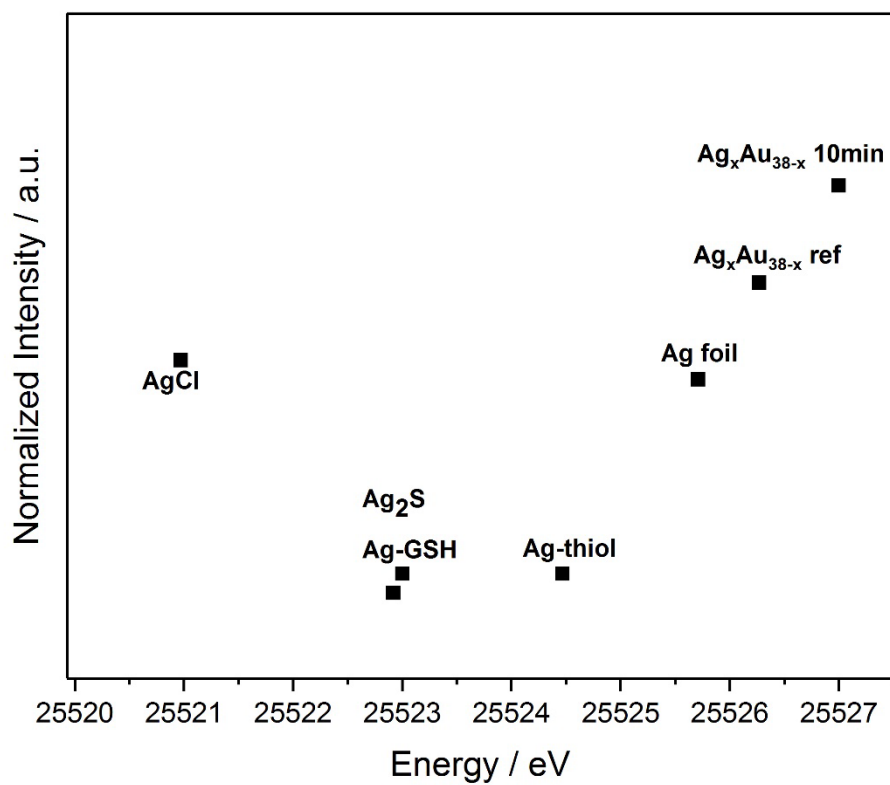


**Figure S4.** White line Energy from XANES spectra of silver references and sample after 10 min reaction at Ag K-edge. <sup>1,2</sup>

1. C. L. Doolette, M. J. McLaughlin, J. K. Kirby, D. J. Batstone, H. H. Harris, H. Ge and G. Cornelis, *Chemistry Central Journal*, 2013, **7**, 46-46.
2. G. Veronesi, A. Deniaud, T. Gallon, P. H. Jouneau, J. Villanova, P. Delangle, M. Carriere, I. Kieffer, P. Charbonnier, E. Mintz and I. Michaud-Soret, *Nanoscale*, 2016, **8**, 17012-17021.